THE HOLE-PRESSURE PROBLEM

by

Dr. M. F. Webster

Numerical Analysis Report No. 2/84

Institute for Computational Fluid Dynamics,
Department of Mathematics,
University of Reading,
Whiteknights, Reading, RG6 2AX, UK.

with one figure and five tables.

SUMMARY

There is a need to unify present hypotheses of the nature and role of the hole-pressure, p_e* , and thus provide consolidation on which to base future research and understanding. This paper is intended to meet this need. Attention is directed towards the calculation of p_e from the velocity and stress fields for viscoelastic fluids flowing across rectangular holes. The constitutive models used are the Newtonian, Second-order and Maxwell models, for values of Reynolds number up to 10 and Weissenburg number up to 0.1.

The numerical complications involved are studied through an investigation of the constituent parts of p_e. Verification of present theory is then sought, from which justification may be derived for the estimation of elasticity from p_e measurements. Attention is directed towards the predictions of Higashitani and Pritchard (3) and the extension to the Tanner and Pipkin theory for 'Second-order' fluids (1). The effects of variation of geometric dimensions and flow type upon p_e are also discussed.

---

* Or hole-pressure error, defined as $p_e = p_b - p_a$ where p_b is the pressure measured at the base of a liquid-filled hole and p_a is that which would be exerted on the channel wall by a flowing liquid in the absence of the hole.

1. Introduction

The interest expressed in the hole-pressure arises through the claim that this quantity plays an important part in the simple yet reliable prediction of the material properties of viscoelastic liquids. This study is important both from a theoretical and experimental standpoint, to resolve what has proved to be a highly controversial issue (see, for example, the experimental findings of some workers (4-8) and the comments of others (9)). The papers of Tanner and Pipkin (1), Kearsley (2) and Higashitani and Pritchard (3) provide the relevant theoretical background. It is suggested that the hole-pressure may be a useful quantity to measure providing estimates of the first, ν_1 , and second, ν_2 , normal-stress differences of a liquid in unidirectional shear flow. There is also some evidence to indicate that variation in molecular weight distribution can affect p_e more significantly than the viscosity (10). These observations reveal the practical role that p_e and its measurement takes, in monitoring polymerization reactions and providing a measure of elasticity during polymer melt processing (11,12).

Tanner and Pipkin have presented an analysis for the creeping flow of Second-order (SOE) fluid models <u>across</u> rectangular holes such as in figure 1.* They established a simple relationship between the first normal-stress difference and the hole-pressure given by

$$p_e = - 0.25 \nu_1^a , \qquad (1)$$

where a denotes the location shown in fig. 1.

The following important assumptions are made in the derivation of equation [1]:

(i) the streamlines are symmetrical about the hole-centreline;

(ii) the hole-width, ℓ_2 , is sufficiently narrow and the hole-depth, ℓ_3 , sufficiently deep to provide stagnation at the base, to ensure that fully-

---

* Poiseuille flow is driven by a pressure gradient, whilst Couette flow is driven by a moving-plate AH.

developed flow does not occur on the centreline and that the presence of the hole has negligible effect upon the opposing channel wall.

The relevance of these assumptions is discussed under various flow conditions. Tanner and Pipkin justified the negative p_e value for an elastic liquid using a force balancing argument (see (1)).

Kearsley derived a result similar to equation [1] relating the hole-pressure to the second normal-stress difference for the slow rectilinear flow of Newtonian and Second-order model fluids, along slots placed parallel to the main flow direction. Higashitani and Pritchard confirmed the results of Tanner and Pipkin, and Kearsley, using a slightly different approach based upon kinematic considerations, and went further extending their analysis to a wider class of materials. This analysis extended that of Kearsley to the rectilinear motion of any material. Extension of the Tanner-Pipkin theory is, however, only an approximation; it is exact for slow flows of Newtonian and SOE fluids. Similarly Higashitani and Pritchard also proposed an approximate result for shear flows across circular holes relating p_e to $\frac{1}{6}\left(\nu_1^a - \nu_2^a\right)$.

The assumptions made within the Higashitani-Pritchard analysis prove, however, to be quite severe. Crucial dependence is placed upon the symmetry of the streamline patterns about the hole-centreline. These requirements are indeed met for Stokesian flows across any symmetrical cavity and hence, likewise for creeping SOE flows at least in two-dimensions (see Tanner's theorem (13)). This is also true when a symmetrical recirculating region occurs within the hole, as observed by this and other authors (7,14); there is disagreement here with the work of Han and Yoo (15) however. Later it is shown how this symmetry is lost, both due to fluid inertia and elasticity effects, which leads to an investigation upon the bearing this has on equation [1].

It is the aim of this paper to compute p_e for various viscoelastic fluid flows, concentrating upon steady flow across rectangular holes. Hole-pressure is calculated from the velocity and stress fields provided by the finite-difference numerical methods outlined by Davies and Webster (19) and confirmed by the flow visualization work reported in Cochrane et al. (17). The particular constitutive models used are Newtonian, Second-order and implicit Maxwell/Oldroyd differential models (see (16-18) for justification). The assumed equations of state are then

$$p^{ik} = - p\delta^{ik} + p'^{ik} \qquad [2]$$

$$p'^{ik} + \lambda_1 \frac{\mathcal{D} p'^{ik}}{\mathcal{D} t} = 2\eta_o \left[1 + \lambda_2 \frac{\mathcal{D}}{\mathcal{D} t}\right] e^{(1)ik} \qquad [3]$$

where standard tensor notation is used throughout, δ^{ik} is the Kronecker delta, p is an isotropic pressure, $e^{(1)ik}$ is the (first) rate-of-strain tensor and $\frac{\mathcal{D}}{\mathcal{D} t}$ is the convected time derivative introduced by Oldroyd (20). Such models give non-zero first normal-stress differences and are restricted to a constant viscosity η_o. λ_1 is a relaxation time and λ_2 is a retardation time (where $\lambda_1 \geq \lambda_2 \geq 0$); $\lambda_1 = \lambda_2 = 0$ yields the Newtonian model, $\lambda_1 = 0$ the SOE model and $\lambda_2 = 0$ the Maxwell model. Of course $\lambda_1 \neq 0$, $\lambda_2 \neq 0$ provides the so-called Oldroyd 'B' model.

It is convenient here to define two dimensionless numbers, the Reynold's number R , and an elasticity (Weissenberg) number, W , as follows:

$$R = \rho \frac{\overline{U}L}{\eta_o} \quad \text{and} \quad W = \left(\lambda_1 - \lambda_2\right) \frac{\overline{U}}{L} \quad , \qquad [4]$$

where ρ is the density, $\overline{U}$ is a characteristic velocity (the mean velocity over the inlet AB) and L is a characteristic length (the channel-width ℓ_1).

2. Calculation of the Hole-pressure

The basic equations from which the pressure solution $p(x,y)$ is derived are the stress equations of motion. These may be non-dimensionalized as outlined in Cochrane et al. (17). For a steady incompressible two-dimensional fluid flow in rectangular Cartesian coordinates (x,y) without body forces these may be written as:

$$\frac{\partial p}{\partial x} = - R\left[u\frac{\partial u}{\partial x} + v\frac{\partial u}{\partial y}\right] + \frac{\partial p'^{xx}}{\partial x} + \frac{\partial p'^{xy}}{\partial y} , \qquad [5]$$

$$\frac{\partial p}{\partial y} = - R\left[u\frac{\partial v}{\partial x} + v\frac{\partial v}{\partial y}\right] + \frac{\partial p'^{xy}}{\partial x} + \frac{\partial p'^{yy}}{\partial y} , \qquad [6]$$

where the velocity vector $\boldsymbol{v} = (u,v)$ and p'^{ik} are the components of the contravarient extra-stress tensor. For future reference, the extra-stress tensor is subdivided into separate non-Newtonian and Newtonian additional constituents as follows:

$$p'^{ik} = S^{ik} + 2e^{(1)ik} \qquad [7]$$

The undisturbed wall thrust p_a is associated with the value $- p^{yy}$ at an appropriate point on the hole-centreline , ab , far out in the mainstream channel flow as illustrated in fig. 1. With a similar identification for the pressure p_b in the stagnation region at the hole-bottom , p_e , may then be calculated as follows:

$$p_e = p_a^{yy} - p_b^{yy} . \qquad [8]$$

Utilising equation [2] and equation [6] and integrating along the unique hole-centreline path produces the following result:

$$p_e = \int_a^b - \frac{\partial p^{yy}}{\partial y} dy = \int_a^b \left\{ - R\left[u\frac{\partial v}{\partial x} + v\frac{\partial v}{\partial y}\right] + \frac{\partial p'^{xy}}{\partial x}\right\} dy$$

or

$$p_e = \int_a^b \left\{ \underbrace{- R\left[u\frac{\partial v}{\partial x} + v\frac{\partial v}{\partial y}\right]}_{\text{term [1]}} + \underbrace{\left[\frac{\partial^2 u}{\partial x \partial y} + \frac{\partial^2 v}{\partial x^2}\right]}_{\text{term [2]}} + \underbrace{\left[\frac{\partial S^{xy}}{\partial x}\right]}_{\text{term [3]}} \right\} dy . \qquad [9]$$

Initially, creeping flow conditions are analysed. Stokesian flow displays a symmetrical streamline pattern, irrespective of the presence of a recirculating (or secondary) flow region in the hole. Hence under such conditions the prevailing kinematical fields show p_e completely determined by term [2] of equation [9], yielding a vanishing value as consistent with the Tanner-Pipkin theory. In addition, for the creeping flow of SOE fluids with an identical (Newtonian) velocity field, p_e is totally determined by term [3] of equation [9]. The implications are clear: that the shear stress p^{xy} is symmetrical† about the centreline ab to a first-order approximation, but need not be at second-order level, where p_e is determined solely by S^{xy}. Beyond second-order behaviour p_e will be effected by both terms [2] and [3] of equation [9], and the flow pattern may then lose its symmetry about ab. The contribution from term [2] will, in general, no longer vanish though it will, in the absence of inertia, often prove to be an order of magnitude lower than term (3). Finally, when inertial effects are also significant, term (1) will also contribute to p_e. The dual disturbances of inertia and elasticity upon the flow pattern, and therefore upon p_e, are now apparent. The question remains whether or not these changes can be related to present theory.

The integrations involved in equation [9] are computed using the Trapezoidal or Simpson's quadrature rule. Hole-pressure results are presented in tables 1 - 5 for both the square and narrow hole geometries, and for Poiseuille-type and Couette-type flows. In tables 1 - 4 a range of R values is considered ($0 \leq R \leq 10$), and for each R value p_e results are recorded for the Newtonian ($W = 0$), SOE ($W = .025$) and Maxwell ($W = .025$, $.05$, $.1$) models. Table 5 compares p_e values for Newtonian liquids and values of R up to 10.

---

† The Newtonian shearing stress is an even function of x about the centreline in the absence of inertia (cf. (1)).

The discrete numerical solutions obtained in Davies and Webster (19) (see also (16 - 18)) are provided on a square finite-difference grid, permitting the use of twenty mesh lengths h across the main unit channel-width, ℓ_1. The selected hole dimensions are then $\ell_2 = \ell_3 = \ell_1$ in the square hole case, and $\ell_3 = \ell_1$ with $\ell_2 = \ell_1/2$ in the narrow hole variety. In all instances a hole-depth $\ell_3 = \ell_1$ is found quite adequate to provide stagnation at the bottom of the hole.

3. Discussion of the results

The results are discussed in the light of the published literature, indicating the main points of computational difficulty and the manner in which they are overcome. Numerical solutions for p_e calculations have been found by Malkus (21) for the creeping flow of SOE fluids. This work presented results for the ratio $p_e : \nu_1$ as a function of depth: width ratio of the hole, both for Poiseuille and Couette flows. The numerical method used is the finite element method (FE) though the flow conditions are restricted to $R = 0$ only. More recently, Crochet and Bezy (22) have used a new finite element technique to study Poiseuille flow of both Newtonian and Maxwell-type fluids across holes. Only a limited number of these results are given, over which the authors express their concern due to the numerical error involved. These provide an extension to the range of inertia and elasticity beyond creeping flow and second-order behaviour respectively. Townsend (23) has also done some similar work using finite difference techniques (FD) to investigate the Poiseuille flow of a SOE fluid (at fixed W) across various shaped rectangular holes for a range of inertial values. This work has been extended by Richards and Townsend (24) recently to also cover implicit Oldroyd-type models (see also Jackson and Finlayson (25) for further reference).

The results of the present study are catalogued in tables 1 - 5, where use is made of a correction for the inertial and Newtonian terms to compute a ratio θ, based upon the relationship in equation (1) (cf.(23,24)). All present hole-pressure theory relies entirely upon the non-Newtonian term [3] of equation [9]. It is unfortunate that, unlike for the SOE, no general rule exists by which the kinematical terms [1] and [2] may in some sense be correlated for an elastic fluid with those of an "Equivalent" Newtonian fluid. The obvious correction the elastic fluid results would then be simple to achieve. The approach adopted is to compute each individual term of equation [9] and calculate the ratio θ from the third term only. Inspection of the remaining terms provides an indication of the necessity and reliability of the correction used. The ratio θ is defined as

$$\theta = \frac{p_e^{Total} - p_e^{Newt}}{(- \nu_1^{a})} = \frac{Term(3)}{(- \nu_1^{a})} \quad . \qquad [10]$$

It is now a well known result that the corresponding first normal-stress difference for models of type equation [3] in a steady simple shear flow with local shear-rate q (cf.Walters (26)) is

$$\nu_1 = 2Wq^2 \ . \qquad [11]$$

It is important to notice that some discrepancy is expected between the numerically estimated shear-rate q_a on hole-centreline and the theoretically equivalent wall shear-rate in fully-developed flow q_A. Hence, even if assumption (ii) of the Tanner-Pipkin theory is satisfied, it is unreasonable to expect ν_1^a to be equal to ν_1^A. This remark is illustrated by the inclusion of both alternatives in the tables of results.

As mentioned in the assumptions of the Tanner-Pipkin theory, the geometric dimensions of the hole and channel are expected to affect the computation of p_e. The ratio $\ell_2 : \ell_1$ is of crucial importance. This ratio dictates the degree of deviation of the flow about the hole-centreline from fully-developed form. This in turn effects the relative magnitude of $\frac{\partial S^{xy}}{\partial x}$ about the centreline and consequently θ. The observation is made that, under equivalent flow conditions, the narrow hole geometry (in contrast to the square hole variety) always renders less distortion to the symmetrical creeping flow streamline pattern with the introduction of R and W effects. Therefore it is no surprise that the p_e values for the narrow hole case correlate more closely to theoretical predictions than do those for the square hole. In addition, the hole-depth ℓ_3 has relatively little effect upon p_e. The flow proves virtually stagnant beyond a depth about equal to the channel-width ℓ_1. These remarks are all in broad general agreement with the findings of other authors (23,25).

A major complication in the computation of p_e is found to be its relatively small size in contrast to the overall pressure field: typically, $p_e \leq 1\% \ \|p(x,y)\|_\infty$.

This is borne out by the p_e tables of Townsend, where difficulties arising because of small centreline values are overcome by averaging over top-plate and hole-bottom surfaces, thus simulating the pressure transducer's action. The centreline station of application is thus abandoned to attain measurability. This indicated the need for a careful examination of the stress fields involved for different mesh sizes ($h = 0.1$, 0.05) in the present study also. A comparison between the equivalent stress fields for the SOE and Maxwell models under second-order creeping flow conditions (cf. (16,26)) identified the following effects. The relative magnitudes of the normal components p'^{ii} are approximately equal to the non-Newtonian constituent equivalents S^{ii} , which dominate the elastic solution. Such matching deteriorates in the shear stress components p'^{xy} and S^{xy} , where the solution is dominated by the Newtonian contribution leaving S^{xy} an order of magnitude lower than S^{ii}. On a relatively course mesh, a discrepancy is evident in the S^{xy} fields of these two equivalent models and indicates the nature of this major numerical difficulty. It is shown that this complication may be effectively surmounted by the generation of sufficiently refined discrete solutions.

Concentration is centred upon results for the narrow hole and Poiseuille flow to test the Higashitani-Pritchard extension to the Tanner-Pipkin theory. In general these compare favourably with those of other workers (22-25). Under creeping conditions, the theoretical result of $\theta = 0.25$ is obtained to two decimal places for the SOE model at $W = 0.025$, whilst the results for the Maxwell model are $0.22 \leq \theta \leq 0.24$ for $0.025 \leq W \leq 0.1$. Particularly prevalent here is the decrease from the theoretical value as the degree of elasticity increases (cf. table 1). To display numerical noise involved, p_e results are also presented for the SOE model and $R = 0$, using the "Equivalent" Newtonian velocity field. The ratio θ is found to alter negligibly from $R = 0$ to $R = 1$. The streamline patterns are also found to change negligibly for $R \leq 1$ and equivalent models and W values (cf. (17)). This is in agreement with (23) for low W values and (22,24,25) for higher W values. It therefore appears a reasonable experimental approximation to utilise slow flow and an "Equivalent" Newtonian correction to determine p_e for some elastic fluids, and hence also W from tables such as 1-5. Attention is drawn to the θ values generated from q_A and the close proximity of these values to the results of (24), where q_A , and not q_a , is also used.

The situation is somewhat different for the case $R = 10$, where inertia shows significant modification to the streamline patterns. The p_e ratios become $\theta = 0.16$ for the SOE model and for the Maxwell model $0.13 \leq \theta \leq 0.15$ for $0.025 \leq W \leq 0.1$. Crochet and Bezy (22), and Townsend and co-workers (23,24) also report similar findings. The experimental work of Higashitani and Lodge (27) for polymer solutions confirms the credibility of such results i.e. to within 20% of $p_e = -0.18\nu_1{}^A$.

Finally, the departure from the Tanner-Pipkin theory is thus confirmed both due to inertial and elastic effects, with the former proving more dominant under the stated test conditions. Under such conditions, the extended theory of Higashitani and Pritchard is found to be inappropriate, though a close relationship between p_e and ν_1 appears to emerge dependent upon the combination (R,W). The opposing streamline asymmetries generated by inertial and elastic effects can be clearly seen in the flow visualization work of Cochrane et al. (17) (cf. (24) also). This type of asymmetrical response due to elasticity is reported but not understood by Hou et al. (14).

These conclusions agree with the current work of Malkus and co-workers (28), who have approached the problem from a different slant, namely the direct study of the Higashitani-Pritchard integral relationship between p_e and ν_1. This integral can be related to the Tanner-Pipkin form of equation (1). These workers argue that deviation from the predictions of Higashitani and Pritchard is due to the following: that their calculated history-dependence violates the Higashitani-Pritchard basic assumption that the state of stress on the hole-centreline is one characteristic of a shearing flow. Particle histories are then not shearing histories, even with perfectly symmetrical streamlines, as may conceivably arise when the opposing non-linear effects of inertia and elasticity exactly balance!

The force of this argument is minimised as ideal creeping flow is approached for which the SOE model becomes completely general (cf. (26)), hence justifying slow flow situations yet again.

A recent study has been conducted by Lodge (8) into Newtonian liquid p_e values at small R values. This study is of interest both for testing apparatus design for p_e measurement and for subracting inertial contributions to p_e for non-Newtonian liquids. Lodge summarises the values found by researchers in a table comparing $\hat{p}_e = [-p_e/\sigma_A Re]$ for values of Reynolds number $Re = \rho \ell_2 \ell_1 q_A^2/4\sigma_A$ less than 10 (where σ_A denotes the wall shear stress and $Re = \frac{1}{4} R q_A \ell_2$). The results of the present study for Newtonian liquids are presented in table 5 to facilitate direct comparison. The Poiseuille flow result of $\hat{p}_e = -0.032$ at $Re \simeq 1$ is very close to the calculated values attributed to Crochet, Jackson and Finlayson, and Malkus, though it differs from that of Richards and Townsend. There is also close correlation at $Re \simeq 10$ of the result $\hat{p}_e = -0.024$ with the only result (experimental) quoted by Lodge which is for a circular shaped hole. The Couette flow results of table 5 lie within similar ranges as those for Poiseuille flow, but appear to show little sensitivity to changes in Re and in general, it is felt, cannot be closely relied upon. The overall quality of agreement of the results of table 5 with those of others is very good, with the one exception of the findings attributed to Han and Kim. This is encouraging as far as the determination of realistic inertial corrections to p_e for non-Newtonian liquids is concerned.

The full hole-pressure story emerges from tables 1-5. The effect of hole-width : channel-width ratio is suitably reflected and the decrease in the order of magnitude of the quantities in question for Couette flow is apparent. The Couette flow results reported surprisingly show $^{\theta}q_A$ values closer to theoretical prediction than $^{\theta}q_a$. This anomally arises through the over-estimation of ν_1^a and the small values involved in such instances. It is this author's experience that planar Couette channel flows are a bad test case for numerical p_e calculations. This does not, however, appear to generalise to all Couette flow situations, as shown in the work of Broadbent and Lodge (4).

4. Conclusion

A detailed study of the different contributions to p_e reveals serious numerical difficulties involved in its computation. The Tanner-Pipkin theory is confirmed under creeping flow conditions, whilst the speculative extension of Higashitani and Pritchard receives only limited ratification. There is always departure from the Higashitani-Pritchard theory beyond second-order creeping flow conditions: agreement simply worsens with increase in R and/or W. Taken in combination with an appropriate "Equivalent" Newtonian correction, the Higashitani-Pritchard theory does, however, appear a feasible experimental approximation for slow flows. Hence some justification is derived for the estimation of elasticity from the measurement of p_e for some elastic fluids. A close relationship appears to emerge between p_e and ν_1, though, in general, it is dependent upon the combination (R,W).

The hole-width to channel-width ratio has a significant effect upon p_e, whilst the hole-depth has negligible effect for depths greater than the channel-width. These comments are in broad general agreement with the findings of most other workers in the field. Also avoidance of Couette-type planar channel flows is strongly recommended in p_e calculations due to the severe numerical difficulties that are so often encountered in such contexts.

References

1) Tanner, R.I., A.C. Pipkin, Trans. Soc. Rheol. 13, 471 (1969).
2) Kearsley, A.E., Trans. Soc. Rheol. 14, 419 (1970).
3) Higashitani, K., W.G. Pritchard, Trans. Soc. Rheol. 16, 687 (1972).
4) Broadbent, J.M., A.S. Lodge, Rheol. Acta 10, 557 (1972).
5) Kaye, A., A.S. Lodge, D.G. Vale, Rheol. Acta 4, 368 (1968).
6) Broadbent,J.M., A. Kaye, A.S. Lodge, D.G. Vale, Nature 217, 55 (1968).
7) Lodge, A.S., Patent No.3, 777, 549, US Patent Office (1975).
8) Lodge, A.S., Note J. Rheology, 27(5), 497 (1983).
9) Han, C.D., K.U. Kim, Trans. Soc. Rheol. 17, 151 (1973).
10) Baird, D.G., Ph.D. thesis, U. Wisconsin-Madison (1974).
11) Baird, D.G., A.S. Lodge, RRC Report 27, U. Wisconsin-Madison (1974)
12) Baird, D.G., J. Applied Polymer Sci. 20, 3155 (1976).
13) Tanner, R.I., Phys. Fluids 9, 1246 (1966).
14) Hou, T.-H. P.P. Tong, L. De Vargas, Rheol. Acta 16, 544 (1977).
15) Han, C.D., H.J. Yoo, J. Rheology 24, 55 (1980).
16) Davies, A.R., K. Walters, M.F. Webster, J. Non-Newtonian Fluid Mech. 4, 325 (1979)
17) Cochrane, T., K Walters, M.F. Webster, Phil. Trans. Roy. Soc. Lond. A301, 163 (1981).
18) Walters, K., M.F. Webster, Phil. Trans. Roy. Soc. Lond. A308, 199 (1982).
19) Davies, A.R., M.F. Webster, J. Non-Newtonian Fluid Mech.; to appear (pre-print available).
20) Oldroyd, J.G., Proc. Roy. Soc. Lond. A200, 523 (1950).
21) Malkus, D.S., Proc. VII th Int. Cong. Rheology, Gottenburg, Sweden, 618 (1976).
22) Crochet, M.J., M. Bezy, J. Non-Newtonian Fluid Mech. 5, 201 (1979).
23) Townsend, P., Rheol. Acta 19, 1 (1980).
24) Richards, G.D., P. Townsend, Rheol. Acta. 20, 261 (1981).
25) Jackson, N.R., B.A. Finlayson, J. Non-Newtonian Fluid Mech. 10, 55 (1982).
26) Walters, K., Rheometry-London: Chapman and Hall (1975).
27) Higashitani, K., A.S. Lodge, Trans. Soc. Rheol. 19, 307 (1975).
28) Malkus, D.S., Private Communication.(1983)

Legend

Figure 1.		The Flow Geometry.
Table 1.	p_e v ν_1 :	Poiseuille Flow and Narrow hole geometry.
Table 2.	p_e v ν_1 :	Poiseuille Flow and Square hole geometry.
Table 3.	p_e v ν_1 :	Couette Flow and Narrow hole geometry.
Table 4.	p_e v ν_1 :	Couette Flow and Square hole geometry.
Table 5.	$\hat{p}_e$ v Re :	Newtonian liquids.

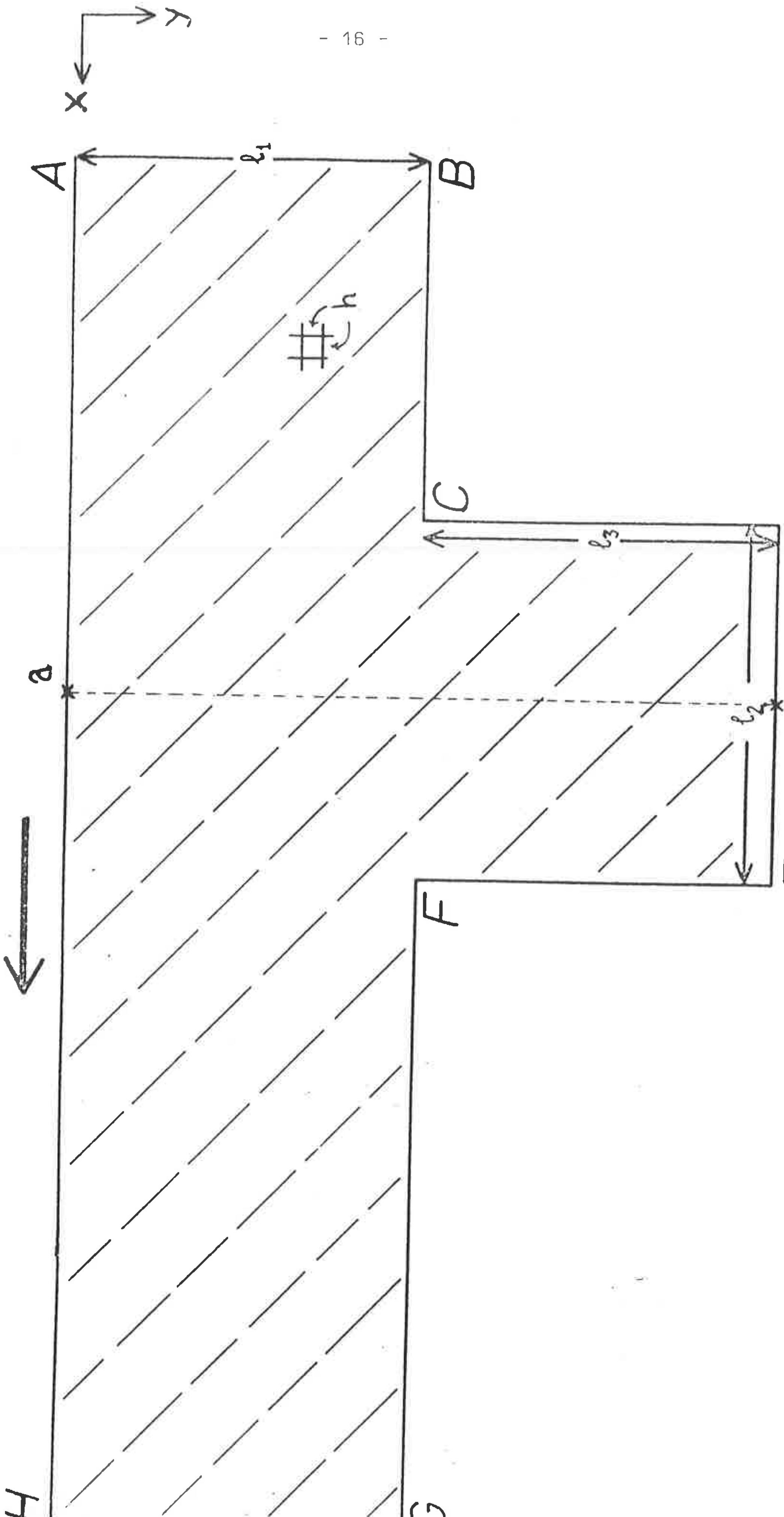

Figure 1. The Flow Geometry

Hole-pressure p_e v first normal-stress difference ν_1

POISEUILLE FLOW   NARROW HOLE GEOMETRY ($\ell_1 = 1$, $\ell_2 = .5$, $\ell_3 = 1$)

FLUID MODEL	THEOR. $(-\nu_1)_A$	NUMER. $(-\nu_1)_a$	p_e: NON-NEWT. NON-INERT. TERM 3	p_e: NEWT. NON-INERT. TERM 2	p_e: NEWT. INERT. TERM 1	θ_{q_A}	θ_{q_a}
NEWT. W=0	0	0	0	-.0037	0	-	-
SOE W=.025	-1.8	-1.6286 -1.6257	-.4037 -.4070	-.0037 .0296	0	.224 .226	.248* .250†
MAX W=.025	-1.8	-1.6259	-.3942	.0168	0	.219	.243
MAX W=.05	-3.6	-3.2506	-.7585	.0012	0	.211	.233
MAX W=.1	-7.2	-6.5079	-1.4563	-.0295	0	.202	.224

(a) R = 0

NEWT W=0	0	0	0	-.1365	.2825	-	-
SOE W=.025	-1.8	-1.6267	-.4054	-.1063	.2848	.225	.249
MAX W=.025	-1.8	-1.6263	-.3907	-.1259	.2854	.217	.240
MAX W=.05	-3.6	-3.2497	-.7575	-.1503	.2895	.210	.233
MAX W=.1	-7.2	-6.4990	-1.4631	-.1704	.2971	.203	.225

(b) R = 1

NEWT W=0	0	0	0	-.8607	2.0539	-	-
SOE W=.025	-1.8	-1.6477	-.2547	-.9618	2.0859	.142	.155
MAX W=.025	-1.8	-1.6479	-.2409	-.9671	2.0811	.134	.146
MAX W=.05	-3.6	-3.2983	-.4420	-1.0583	2.0451	.123	.134
MAX W=.1	-7.2	-6.6044	-.8361	-1.1706	1.9243	.116	.127

(c) R = 10

* Newt. ν Field   † SOE ν Field

TABLE 1

Hole-pressure p_e v first normal-stress difference ν_1

POISEUILLE FLOW SQUARE HOLE GEOMETRY $(\ell_1 = \ell_2 = \ell_3 = 1)$

FLUID MODEL	THEOR. $(-\nu_1)_A$	NUMER. $(-\nu_1)_a$	p_e: NON-NEWT. NON-INERT. TERM 3	p_e: NEWT. NON-INERT. TERM 2	p_e: NEWT. INERT. TERM 1	θ_{q_A}	θ_{q_a}
NEWT W=0	0	0	0	-.0050	0	-	-
SOE W=.025	-1.8	-1.1998	-.2940	-.0050	0	.165	.247
MAX W=.025	-1.8	-1.1987	-.2997	-.0012	0	.165	.247
MAX W=.05	-3.6	-2.3961	-.5866	.0174	0	.165	.247
MAX W=.1	-7.2	-4.7986	-1.1423	.0580	0	.161	.240

(a) R = 0

NEWT W=0	0	0	0	-.2473	.5349	-	-
SOE W=.025	-1.8	-1.1988	-.2919	-.2509	.5389	.164	.245
MAX W=.025	-1.8	-1.1980	-.2901	-.2496	.5399	.163	.244
MAX W=.05	-3.6	-2.3927	-.5807	-.2453	.5476	.163	.245
MAX W=.1	-7.2	-4.7757	-1.1544	-.1922	-.5634	.162	.244

(b) R = 1

NEWT W=0	0	0	0	-1.1696	3.3270	-	-
SOE W=.025	-1.8	-1.2875	-.1145	-1.2483	3.3027	.067	.091
MAX W=.025	-1.8	-1.2879	-.1166	-1.2574	3.2967	.067	.091
MAX W=.05	-3.6	-2.5817	-.2194	-1.3193	3.2462	.063	.087
MAX W=.1	-7.2	-5.1884	-.4007	-1.4348	3.1198	.058	.079

(c) R = 10

TABLE 2

Hole-pressure p_e v first normal-stress difference ν_1

COUETTE FLOW NARROW HOLE GEOMETRY (ℓ_1 = 1 , ℓ_2 = .5 , ℓ_3 = 1)

FLUID MODEL	THEOR. $(-\nu_1)_A$	NUMER. $(-\nu_1)_a$	p_e: NON-NEWT. NON-INERT. TERM 3	p_e: NEWT. NON-INERT. TERM 2	p_e: NEWT. INERT. TERM 1	θ_{q_A}	θ_{q_a}
NEWT W=0	0	0	0	-.0037	0	-	-
SOE W=.025	-.2	-.2146 -.2150	-.0356 -.0359	-.0037 -.0006	0	.178 .180	.166* .167+
MAX W=.025	-.2	-.2146	-.0358	-.0000	0	.179	.167
MAX W=.05	-.4	-.4256	-.072	-.0005	0	.180	.169
MAX W=.1	-.8	-.8384	-.1472	.0009	0	.184	.176

(a) R = 0

NEWT W=0	0	0	0	-.0211	.0385	-	-
SOE W=.025	-.2	-.2150	-.0358	-.0182	.0392	.179	.167
MAX W=.025	-.2	-.2145	-.0356	-.0189	.0395	.178	.166
MAX W=.05	-.4	-.4254	-.0717	-.02	.0398	.179	.169
MAX W=.1	-.8	-.8378	-.1466	-.0194	.04	.183	.175

(b) R = 1

NEWT W=0	0	0	0	-.1386	.3135	-	-
SOE W=.025	-.2	-.2133	-.0274	-.1424	.3144	.137	.128
MAX W=.025	-.2	-.2127	-.0272	-.1451	.3149	.136	.128
MAX W=.05	-.4	-.4217	-.0547	-.1515	.3138	.137	.130
MAX W=.1	-.8	-.8317	-.1135	-.1598	.3111	.142	.136

(c) R = 10

* Newt v Field + SOE v Field

TABLE 3

Hole-pressure p_e v first normal-stress difference ν_1

<u>COUETTE FLOW</u> SQUARE HOLE GEOMETRY $(\ell_1 = \ell_2 = \ell_3 = 1)$

			p_e				
FLUID MODEL	THEOR. $(-\nu_1)_A$	NUMER. $(-\nu_1)_a$	NON-NEWT. NON-INERT. TERM 3	NEWT. NON-INERT. TERM 2	NEWT. INERT. TERM 1	θ_{q_A}	θ_{q_a}
NEWT W=0	0	0	0	-.0028	0	-	-
SOE W=.025	-.2	-.2544	-.0120	-.0028	0	.060	.047
MAX W=.025	-.2	-.2529	-.0125	-.0033	0	.063	.049
MAX W=.05	-.4	-.4975	-.0272	-.0026	0	.068	.055
MAX W=.1	-.8	-.9592	-.0646	-.0029	0	.081	.067

(a) R = 0

NEWT W=0	0	0	0	-.029	.057	-	-
SOE W=.025	-.2	-.2544	-.0119	-.0293	.0572	.060	.047
MAX W=.025	-.2	-.2526	-.0125	-.0297	.0576	.063	.050
MAX W=.05	-.4	-.4964	-.0272	-.0300	.0579	.068	.055
MAX W=.1	-.8	-.9562	-.0649	-.0310	.0583	.081	.068

(b) R = 1

NEWT W=0	0	0	0	-.1555	.3866	-	-
SOE W=.025	-.2	-.2453	-.0047	-.1601	.3839	.024	.019
MAX W=.025	-.2	-.2430	-.0058	-.1618	.3832	.029	.024
MAX W=.05	-.4	-.4781	-.0142	-.1664	.3811	.036	.030
MAX W=.1	-.8	-.9276	-.0375	-.1807	.3752	.047	.040

(c) R = 10

<u>TABLE 4</u>

$\hat{p}_e = \left[\frac{-p_e}{\sigma_A Re}\right]$ v Re for NEWTONIAN LIQUIDS ($\ell_3 = 1$)

$\hat{p}_e$	Flow Type and Hole Shape	$Re = \frac{1}{4} R q_A \ell_2$	R	ℓ_2/ℓ_1
-0.032	Poiseuille - Narrow hole	0.75	1	0.5
-0.027	Poiseuille - Narrow-hole	7.5	10	0.5
-0.032	Poiseuille - Square hole	1.5	1	1
-0.024	Poiseuille - Square hole	15	10	1
-0.035	Couette - Narrow hole	0.25	1	0.5
-0.035	Couette - Narrow hole	2.5	10	0.5
-0.028	Couette - Square hole	0.5	1	1
-0.023	Couette - Square hole	5.0	10	1

TABLE 5

Acknowledgments

I would like to thank Dr. A. R. Davies and Professor K. Walters, Applied Mathematics Department, University College of Wales, Aberystwyth, U.K., for their helpful support during the period of this work. I am also indebted to Dr. P. Townsend, Computer Science Department, Swansea University, U.K., for his invaluable assistance in the drafting and preparation stages, and to Dr. D. S. Malkus, Department of Mathematics, IIT, Chicago, U.S.A., for his relevant and instructive comments in a most recent private communication. Financial support from the Science Research Council, GB is gratefully acknowledged for part of the time spent upon this work.